Handling contact points in reactive CFD simulations of heterogeneous catalytic fixed bed reactors

Stefano Rebughini [a], Alberto Cuoci [b], Matteo Maestri [a,*]

[a] *Laboratory of Catalysis and Catalytic Processes, Dipartimento di Energia, Politecnico di Milano, Piazza Leonardo da Vinci 32, 20133 Milano, Italy* [b] *Department of Chemistry, Materials and Chemical Engineering, Politecnico di Milano, Piazza Leonardo da Vinci 32, 20133 Milano, Italy*

A B S T R A C T

The mesh generation is a crucial step for Computational Fluid Dynamic (CFD) simulations and incorrect numerical descriptions of the geometry may strongly affect the reliability and the accuracy of the results. This is especially true in handling the contact points in random packed bed of spheres. In this respect, we provide a systematic investigation of the treatment of the contact points for reactive CFD simulations of gas–solid packed beds of spheres. In particular, building on previous literature results on radial heat transfer and pressure drop simulations, we extend and assess the bridge method to reaction at surfaces. At this scope, we first analyze a regular bed of spheres in laminar conditions (Re∼80). This regular packed bed and the laminar flow regime allow for a direct and feasible meshing of the contact points, thus giving the possibility to perform explicit comparisons between meshes with and without bridges. In doing so, we identify guidelines that are then extended and tested to the meshing of a random packed bed reactor. In this way, we identify a meshing protocol, which can be adopted to properly describe surface reactivity in packed bed reactors along with a concomitant sound description of pressure drops and heat transfer.

1. Introduction

Fundamental multi-scale modeling of catalytic reactors is considered as one of the most promising frontier for chemical reaction engineering and is becoming a very powerful tool for the analysis and design of novel and improved catalytic reactor concepts for process intensification (Dudukovic, 2009; Freund and Sundmacher, 2008; Schlereth and Hinrichsen, 2014). Contrary to classical and phenomenological methodologies, this approach is based on the simulation of the reactor behavior by means of parameters and descriptors, which are directly linked to theore-tical accessible phenomena. At this level of description, the detailed analysis obtained via a fundamental multi-scale analysis provides peculiar insights either to help the interpretation of experiments or to rationally derive lumped parameters to be used

A R T I C L E I N F O

Article history:
Received 30 April 2015
Received in revised form
25 October 2015
Accepted 18 November 2015
Available online 1 December 2015

Keywords:
Computational Fluid Dynamics
Discrete Element Method
Fixed bed reactors
Contact points
Gas–solid reactor
Catalysis

H I G H L I G H T S

- The problem of contact points in reacting CFD of gas–solid reactors is assessed.
- The bridge method is extended to the situation of reaction at surfaces.
- A meshing protocol for surface chemistry in packed bed reactors is presented.

G R A P H I C A L A B S T R A C T

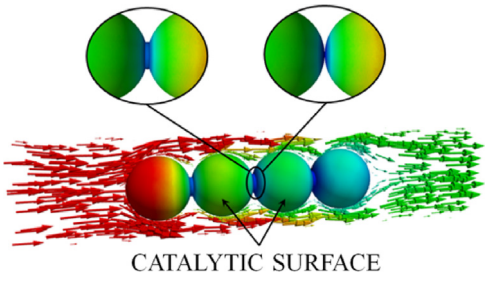

* Corresponding author.
E-mail address: matteo.maestri@polimi.it (M. Maestri).

Published Journal Article available at: http://dx.doi.org/10.1016/j.ces.2015.11.013

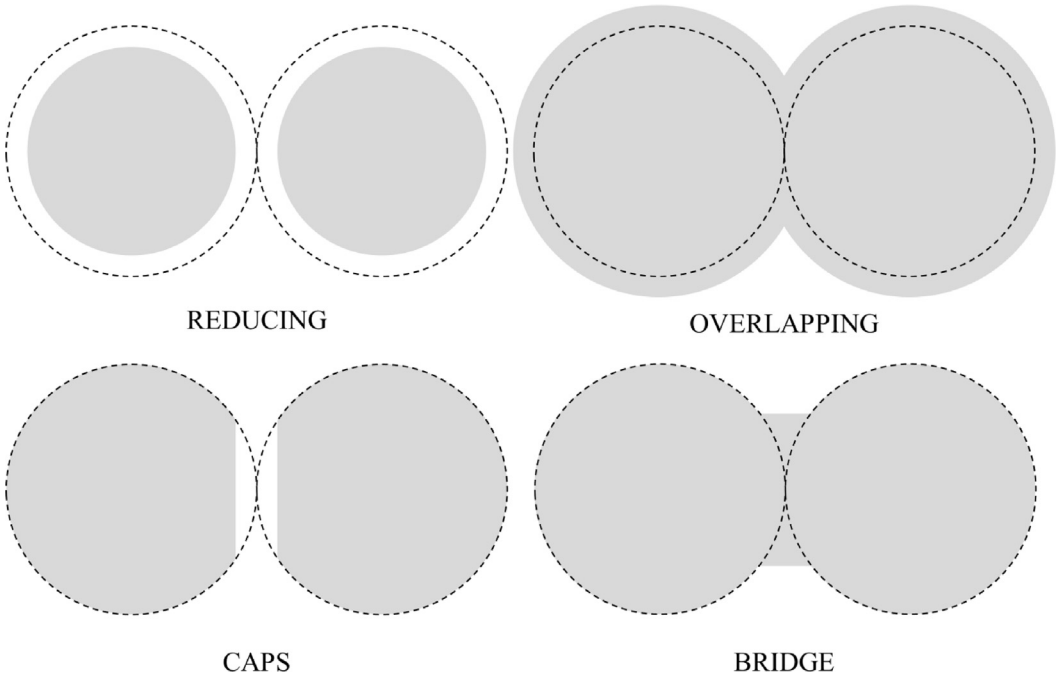

Fig. 1. Schematics of the contact point modifications, after Dixon et al. (2013).

in lower hierarchy models (Raimondeau and Vlachos, 2002; Schlereth and Hinrichsen, 2014). Typical reactors for heterogeneous reactions are fixed beds, foams, or multi-channel reactors. In this regard, Computational Fluid Dynamics (CFD) simulations are acknowledged to be the enabling tool for the fundamental assessment of the transport properties in the reactor, by providing a detailed description of the flow field in the different reactor geometries (Dixon and Nijemeisland, 2001). These simulations, however, strongly rely on the proper description of the geometry in terms of computational domain, which – if not properly accounted for in the simulations – may invalidate the results of such enormous effort. In particular, a crucial issue is related to the construction and proper meshing of the complex computational domain of randomly-packed fixed bed reactors (Dixon et al., 2013; Eppinger et al., 2011). These computational domains are typically generated either by using computational methodologies, which mimic the actual generation of a packed bed, or by relying on non-invasive imaging reconstruction of real packed beds (Baker et al., 2011), such as the magnetic resonance image (MRI). For the computational generation of packed beds, the most common techniques are the Discrete Element Method (DEM), which was first described by Cundall and Strack (1979), and the two-step Monte Carlo methods proposed by Soppe (1990) and adopted by Freund et al. (2005, 2003). Once the random geometry is created, the computational domain has to be meshed, i.e., subdivided in small control volumes. The main issue associated with the mesh generation for random packing is the description of the spheres and the generation of the mesh close to the contact points. Most of the literature agrees that the contact point description represents a crucial numerical problem for CFD simulation of fixed packed bed reactors (Augier et al., 2010; Bu et al., 2014; Calis et al., 2001; Dixon et al., 2013, 2010; Eppinger et al., 2011; Guardo et al., 2006; Jiang et al., 2006; Ookawara et al., 2007; Romkes et al., 2003). When the fluid mesh near the wall–particle and the particle–particle contact points is created, the cells become very skewed. This leads to numerical problems, which prevent from the convergence of the flow field solution. Only a small number of studies report meshes of three dimensional packed beds of spheres without any alteration of the extremely narrow regions in proximity of the contact points (Lund et al., 1999; Magnico, 2003; Touitou et al., 2014). For instance, Magnico (2003) states that the use of structured mesh avoids contact points, but he also reported that strict mesh-independence was not achieved, despite the huge number of cells employed (17.7 million cells) for a bed of 620 particles. Touitou et al. (2014) simulated beds with a large number of spheres ($\sim$3000) in adiabatic reactive conditions and in laminar regime ($Re < 30$). However, the mesh reported in the paper reveals a poor quality of the description of the spheres and contact points, which may substantially affect the CFD results. Thus, it is clear that a fine description of the spheres and contact points with a concomitant acceptable skewness of the mesh is required to achieve a sound simulation result. In this respect, four different techniques are adopted and presented in the literature for a computationally affordable description of the contact points, as shown in Fig. 1. In particular, Dixon et al. (2013) analyzed these approaches to draw guidelines for the systematic meshing of fixed bed reactors, with particular attention to pressure drops, void fraction, and heat transfer. They distinguish between global (where the whole sphere geometry is modified) and local methods, (where the spheres are modified only near the contact points). The reducing approach was proposed by Calis et al. (2001), Romkes et al. (2003) and Dixon and Nijemeisland (2001): spheres at 99–99.5% of their nominal diameter are used to remove the contact between them. The overlap approach was adopted by Guardo et al. (2006) by extending the sphere diameter to allow for a 1% overlap between two touching spheres. A similar method was used by Jiang et al. (2006) with the creation of small contact areas instead of the contact point for micro-porous spheres. Ookawara et al. (2007) proposed to insert

Table 1
Input parameters for the DEM simulations.

Particle density	2500 kg/m^3
Restitution coefficient	0.2
Young module	10^6 N/m^2
Poisson ratio	0.45
Friction coefficient	0.15

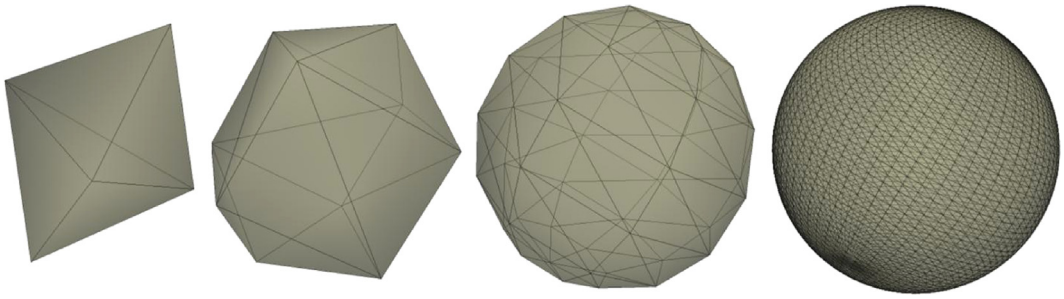

Fig. 2. Description of a sphere with the Standard Tessellation Language (STL).

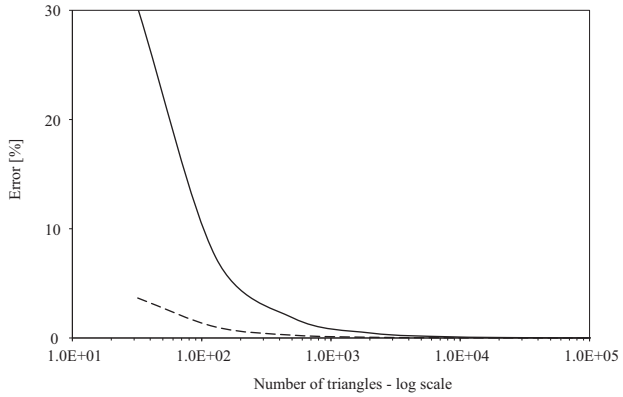

Fig. 3. Error on the volume and the surface of a single sphere for the STL file as a function of the number of triangles. Solid line is the surface. Dashed line is the volume.

cylinder between every spheres, with its axis oriented along the center-to-center line of the spheres. This technique is known as bridge method and the bridge dimensions can be characterized by the bridge-to-particle diameter ratio. Recently, Eppinger et al. (2011) proposed the caps method. The sphere surface is modified by introducing a gap between the points of two different contacting spheres, thus resulting in a local flattening of the particles that can avoid the generation of skewed cells. Dixon et al. (2013) suggested that a reasonable description of both the void fraction and pressure drops can be obtained only by using the local modification of the bed, as occurs with the caps and the bridge method. Moreover, the bridge technique, in contrast with caps, is also very suitable to describe heat transfer between two spheres by setting proper bridge conductivity. Thus, the bridge method turns to be the most suitable technique for a proper description of void fraction, pressure drops, flow field, and heat transfer in random packed bed reactors. The analysis carried out by Dixon et al. (2013) was focused on the heat transfer and the pressure drops, without taking into account the reactivity. Nevertheless, the modification of the mesh due to the presence of the bridges between the contact points provides a modification of the surface area, which may substantially affect the surface reactivity. Therefore, the aim of this work is to extend the analysis to the assessment of the influence of the bridge method on the reactivity of packed bed reactors. This, in conjunction with the previous work reported by Dixon et al. (2013), can be considered the essential step to set a protocol for the proper meshing of random packing to be used for the detailed analysis of heterogeneous catalytic fixed bed reactors.

The paper is organized as follows. In the first part, we assess the effect of the introduction of the bridges by considering the ideal situation of a regular packed bed in laminar conditions (Re$\sim$80). This regular packed bed and the laminar flow regime allow for a direct and feasible meshing of the contact points and thus make possible an explicit comparison between meshes with and without bridges. This ideal configuration helps us in identifying guidelines that are then extended and tested to the meshing of a random packed bed reactor. In doing so, we establish specific guidelines for bridging the contact points without affecting neither the reactivity nor the transport properties of the bed.

2. Methods

2.1. Random packing generation

The generation of the random packing is carried out with the implemented DEM in the open source CFD-DEM code LIGGGHTS (Kloss et al., 2012). Spherical particles are randomly initialized in a square section tubular domain where they fall due to the gravity force. The momentum equations, which take into account for the forces and the interaction between particles, are solved until the velocity of all the particles is virtually zero. The input parameters for the DEM simulations are reported in Table 1.

2.2. Mesh generation

For the mesh generation, particle data (position of the centroid) of the finished DEM simulations are imported into the open source multiple-platform ParaView application (Henderson, 2007) and the packed bed of spheres is created using the Standard Tessellation Language (STL). Moreover, the particle data are also used to find the contact point positions. The contact points between the spheres can be estimated by considering all the centroid that have a distance equal to the sphere diameter from the selected one. The DEM simulation, for its nature, generates non-perfect contact points between the spheres, thus the centroid distance is evaluated with a relative tolerance of 0.001. Then the middle distances between these points, that are the contact points, can be estimated. Finally, the bridges are directly added into the STL file at these positions. The STL describes the surface of solids using triangles and all the spheres are described by increasing the number of triangles of two tetrahedrons, as shown in Fig. 2, until reaching a correct description of volume and surface. Fig. 3 shows the errors on the sphere surface and volume as a function of the number of triangles on the STL surface. The errors are estimated as the difference between the volume and surface analytically calculated and the ones from the STL file. This definition leads to Eqs. (1) and (2)

$$\varepsilon_V^{STL} = \left| \frac{\frac{\pi \cdot D_p^3}{6} - V_{STL}}{\frac{\pi \cdot D_p^3}{6}} \right| \cdot 100 \tag{1}$$

$$\varepsilon_A^{STL} = \left| \frac{\pi \cdot D_p^2 - A_{STL}}{\pi \cdot D_p^2} \right| \cdot 100 \tag{2}$$

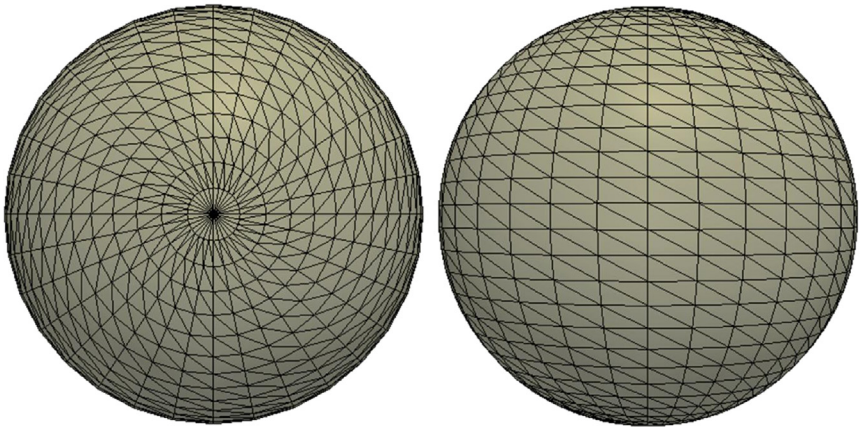

Fig. 4. Poles of a sphere described with an STL file.

One relevant property of the spheres, described with a STL file, is that all the edges of the triangles start from two different points, which can be considered as poles, as shown in Fig. 4. These poles are relevant to obtain an exact description of the contact points, by making the spheres touch each other in the poles of the STL. In this regard, the poles of the STL file have to be exported in the mesh. To this aim, a cut-cell approach, where the mesh approximately conforms the surface by iteratively refining without using the vertices of the triangles as starting points, cannot be applied. Instead, a boundary-conforming mesh is mandatory to directly export the geometrical properties of the STL file into the fluid mesh. This approach creates the cells near the surface starting from the vertices of triangles of the STL file. The mesh, based on tetrahedrons, "grows" from the surface of the STL file. For these reasons, we generate all the computational grids using the open source TetGen code (Si, 2007). An example of the resulting mesh is reported in Fig. 5, which shows that, due to the laminar flow conditions, no prism layer is created near the walls of the spheres.

2.3. Model

The reactive CFD simulations are carried out with the catalyticFOAM solver (Maestri and Cuoci, 2013). This solver describes the fluid and the chemistry on the surface of the catalyst. The mass flux of the individual species is assumed equal to the formation rate due to the heterogeneous reaction occurring on the catalytic wall. Thermal and gas properties are estimated according to the CHEMKIN correlations (Appel et al., 2005; Kee et al., 1990; Reid et al., 1987) implemented in the OpenSMOKE++ libraries (Cuoci et al., 2015), which is incorporated into the catalyticFOAM framework. Accordingly to the operator splitting approach (Maestri and Cuoci, 2013), during the time integration, the reaction terms is separated from the transport process and the numerical integration is performed with different numerical solvers. In particular, the reaction terms are integrated in time using the OpenSMOKE++ ODE solver (Cuoci et al., 2015), which is specifically conceived for stiff ODE systems describing reactive conditions. On the contrary, the momentum equations and transport terms are solved with the solvers implemented in OpenFOAM® framework (Jasak et al., 2007). A more detailed description of the numerical method and the solved equations are reported in (Maestri and Cuoci, 2013). Moreover, a non-slip and a Neumann boundaries conditions ($\nabla(\cdot)=0$) are applied to the velocity and pressure fields, respectively, at the catalytic wall.

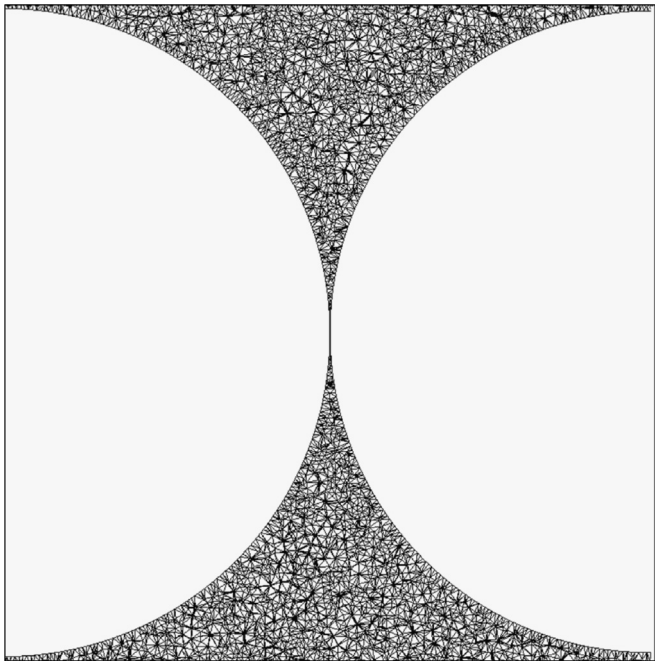

Fig. 5. Mesh near the contact points.

3. Results and discussions

In order to investigate in detail the effect of bridging the contact points on the reactivity, we first focus our attention to a regular packed bed made of 4 spheres (see Fig. 6a). This configuration – due to its regular geometry – can be meshed also without any treatment of the contact points, thus making possible a benchmark for the bridge method through an explicit comparison between meshes with and without bridges. We assess the effect of the bridging on the reactivity by analyzing different bridge-to-particle diameter ratios. Thus, we identify limits for the bridge-to-particle diameter ratio, which do not introduce relevant differences with respect to the reference mesh without any treatment of the contact points. Then, the analysis is extended to a random packed bed of spheres, which cannot be meshed with an exact description of the contact points, due to the randomness of the contacts between the spheres.

3.1. Regular bed

Two regular packed beds with a low number of spheres, whose dimensions are reported in Table 2, are designed for a detailed

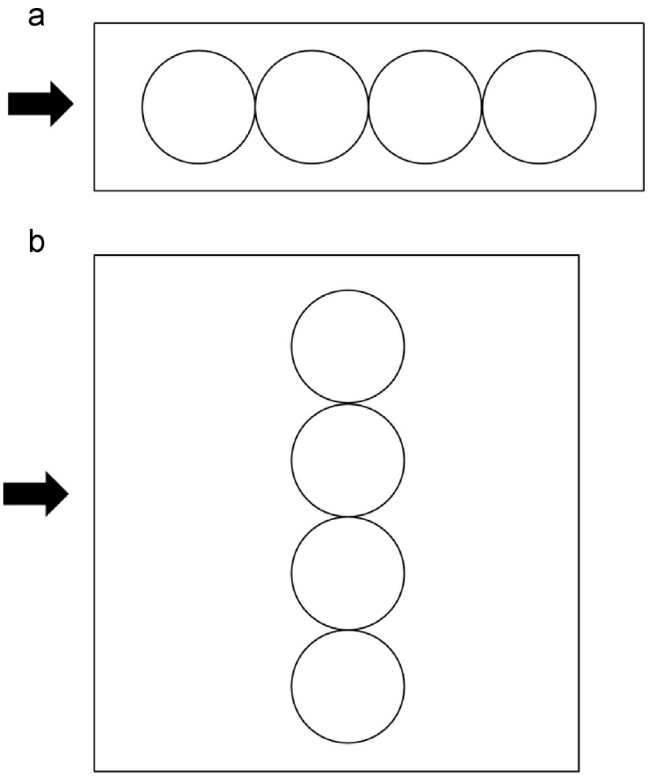

Fig. 6. Regular packed bed reactors configurations. (a) Convective flux parallel to bridge axes and (b) convective flux normal to bridge axes.

Table 2
Regular packed bed dimensions.

	Configuration A	Configuration B
Axial length	0.44 m	0.70 m
Side length	0.10 m	0.30 m
	0.10 m	0.08 m
Sphere diameter	0.06 m	0.06 m

analysis of the effect of the bridges on the system reactivity. These configurations, shown in Fig. 6, are chosen to represent the two possible conditions of flow impact on the bridges. Indeed, the axis of the bridge is parallel to the flow field in configuration A, and it is normal to the flow field in configuration B. These layouts are considered as the two asymptotic conditions of flow impact on the bridges present in a random packed bed reactor and they are selected for the systematic analysis of the bridge influence.

To assess the effect of the bridging on the system reactivity we first create a mesh without local modifications by exploiting the pole-to-pole contact between the spheres. Due to the laminar flow conditions, reported in Table 3, a prism layer is not required for correctly describe the flow field, thus a mesh without any treatments of the contact points can be successfully generated. This mesh is then used as the reference in order to quantify the effect of bridging the contact points. In Fig. 7 the specific catalytic area is reported, evaluated according to Eq. (3)

$$a_V = \frac{A_C}{V_R} \tag{3}$$

The catalytic area (A_C) is calculated from the meshes for the packed bed shown in Fig. 6a. On the contrary, the geometric value is estimated by considering the surface of the four spheres as catalytic area. In Fig. 7 the specific catalytic area is plotted against the refinement level. The refinement level for this meshing procedure is controlled by the selected maximum cell volume. Fig. 7

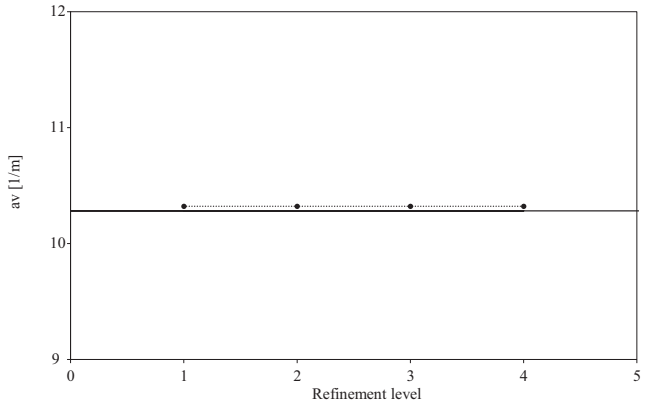

Fig. 7. Analysis of catalytic area for the regular packed bed. Circular points and point line: meshed value; solid line: geometric value.

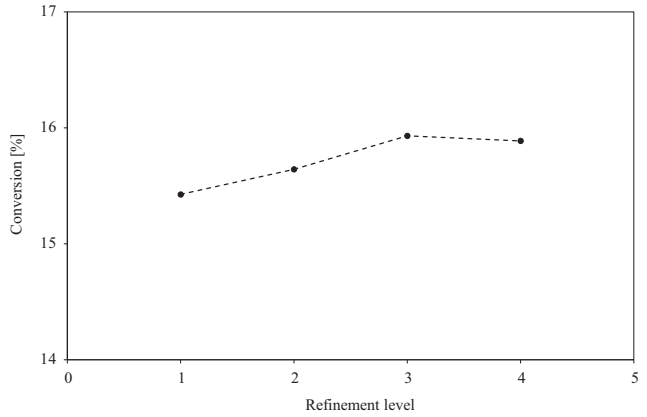

Fig. 8. Mesh independence analysis for regular packed bed.

shows that the difference between the calculated catalytic area and the geometrical value is close to zero (0.4%), and it is constant for all the mesh refinement levels. For a boundary conforming mesh the poles are the "source" for all the cells near the contact points. Therefore, the mesh can correctly describe the contact points and the narrow volume between spheres. Moreover, a boundary conforming mesh allows removing the problem of the skewed cells near the contact points. Indeed, the cells near the contact points "grow" from the points of the STL file and their dimension is small enough to avoid the problem of the skewness.

The two configurations are studied for different bridge dimensions, from a bridge-to-particle diameter ratio of 0.05 up to 0.6. This range is selected to deeply investigate the effect of the bridges on the system reactivity, by comparing the calculated conversion for these beds with those evaluated for the beds without any treatment of the contact points. The mesh-independence analysis of the conversion and the catalytic area is required to understand the error associated with the employed mesh and to prove that it does not influence the simulation results. This analysis is presented only for the beds without any treatments of the contact points, but the same study has been carried out for all the regular packed beds presented in this work. The operating conditions used also for the mesh-independence analysis are reported in Table 3. Fig. 8 shows that a mesh independent conversion is reached with a refinement level of 3 for TetGen (Si, 2007) (maximum cell volume of 10^{-5} m^3 and 687,650 cells).

The void fraction turns out to be slowly dependent on the bridge-to-particle diameter ratio as shown in Fig. 9a. For instance, the error evaluated according to Eq. (4) for the bridge-to-particle

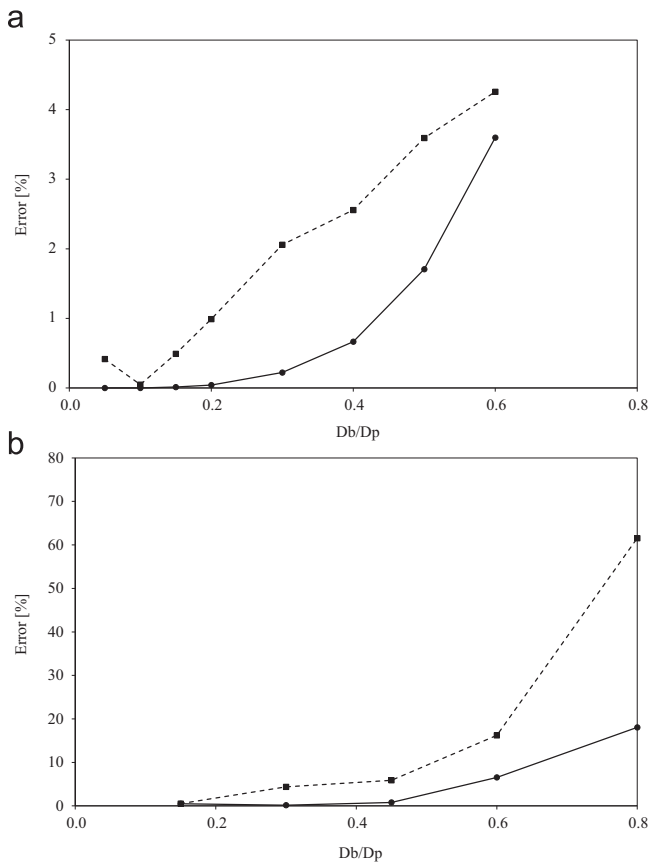

Fig. 9. Geometric effect of bridge dimension (a) on the regular packed bed and (b) on the random packed bed. Dashed line: catalytic area. Solid line: void fraction.

diameter ratio of 0.3 – which is the maximum allowable value for the bridge dimension to ensure a sound prediction of the pressure drops – is smaller than 1%. This can be easily explained by the fact that the number of bridges per spheres are rather limited in this configuration due to the low coordination number (i.e., number of contact points per sphere) of each sphere ($\sim$1).

$$\varepsilon_{void} = \left| \frac{\left(V_R - N_s \cdot \frac{\pi \cdot D_p^3}{6}\right) - V_{mesh}}{\left(V_R - N_s \cdot \frac{\pi \cdot D_p^3}{6}\right)} \right| \cdot 100 \tag{4}$$

For the surface area, two different possibilities can be considered, by describing the bridge area as catalytic or non-catalytic area. In both cases, in contrast with the void fraction, the catalytic area results to be more affected by the presence of the bridges. Fig. 10 shows the comparison of the error associated with the catalytic area, estimated with Eq. (5), for a bed where the bridge area is considered catalytic and a bed where it is non-catalytic.

$$\varepsilon_A = \left| \frac{N_s \cdot \pi \cdot D_p^2 - A_{mesh}}{N_s \cdot \pi \cdot D_p^2} \right| \cdot 100 \tag{5}$$

The bed with catalytic bridges presents a lower error on the catalytic area because the addition of the bridges removes some surface from the spheres, which is partially replaced by the bridge area. Thus, we decided to create beds with catalytic bridges, in order to minimize the geometrical error on the surface area. As shown in Fig. 9a, the overall effect of bridging is higher for the surface area than the void fraction. For instance, a bridge-to-particle diameter ratio of 0.4 results in an error which is at least

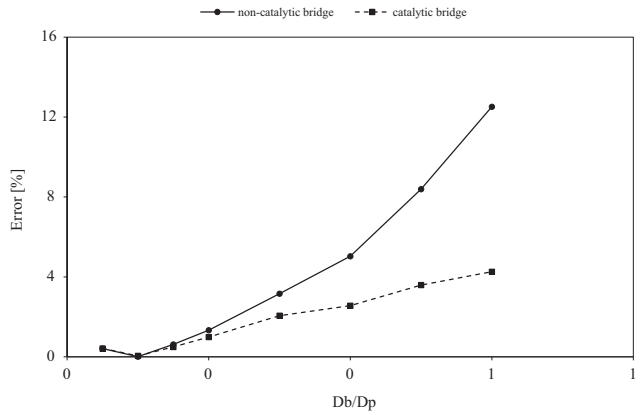

Fig. 10. Comparison of the error on the catalytic area for beds with catalytic bridges (dashed line) and beds with non-catalytic bridges (solid line).

Table 3
Operating conditions.

Operating conditions	
Outlet pressure	1 atm
Temperature	573 K
Feed velocity	0.04 m/s
Reynolds number	$\sim$80

two-times the error for the void fraction (2.5% in case of catalytic bridges).

Then, we explicitly investigate the effect of the modification of the surface area on the overall surface reactivity by performing reactive simulations at different bridge-to-particle diameter ratios. To this aim, we are only interested in the surface reactivity, independently of the specific expression of the reaction rate. Moreover the simulations are carried out in isothermal conditions because the effect of the heat transfer has been already investigated by Dixon et al. (2013) and we focus our attention only to the reactivity at the external surface of the packing, without accounting for mass transfer in the solid. This analysis is carried out by considering a generic first order reaction

$$A \rightarrow B \tag{6}$$

Different values of the reaction constant are considered in order to simulate different Damkholer numbers, from 0.005 (chemical regime) up to 1000 (fully external mass transfer regime). Operating conditions and feed composition are reported in Tables 3 and 4. A bridge-to-particle diameter ratio between 0.05 and 0.3 has been investigated. The upper bound corresponds to the limit found by Dixon et al. (2013) in order to have a correct prediction of the pressure drops. The lower limit, instead, is set by considering the maximum acceptable skewness nearby the contact points. Fig. 11a and b shows the results for the configuration A (the axes of the bridges parallel to the flow direction) and configuration B (the axes of the bridges normal to the flow direction), respectively. These simulations demonstrate that the conversion is not remarkably influenced by the presence of the bridges, despite the error on the surface area in the whole range of bridge-to-particle diameter ratio. Moreover, the effect of the bridges at low Damkholer number, where the global conversion is controlled by the catalytic area, and at high Damkholer number, where it is controlled by external transport limitations, is both analyzed. Table 5 shows that the effect of the bridges in chemical regime as well as in external mass transfer regime on the global conversion is negligible. Finally, to assess the effect of the bridges on the local composition, the axial profile of the cup-mix of the reactant is

Table 4
Inlet composition.

Feed mole fraction	
A	5%
Inert	95%

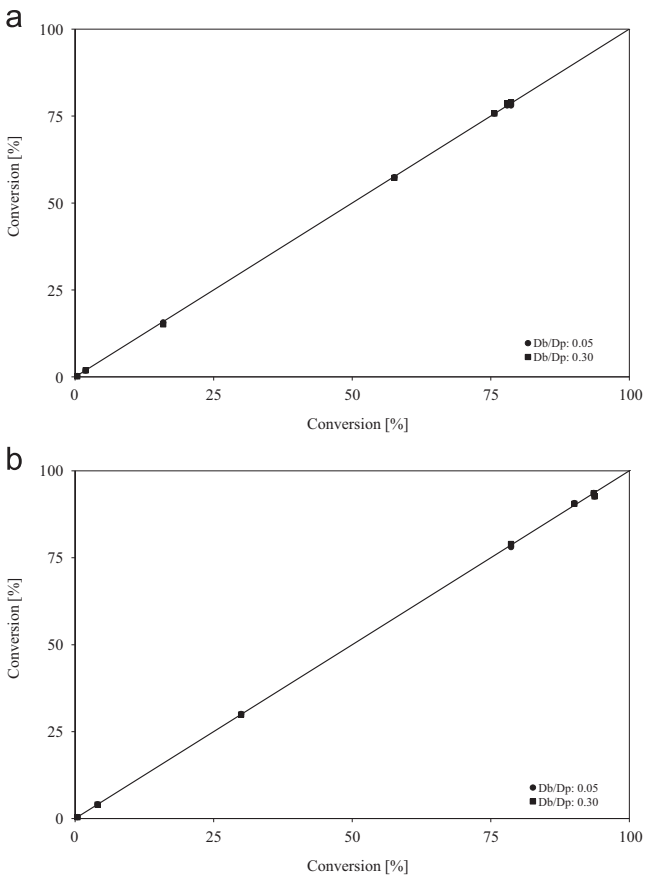

Fig. 11. Parity plot for describing the bridge effect on conversion for different bridge-to-particle diameter ratio: (a) convective flux parallel to bridge axes and (b) convective flux normal to bridge axes.

Table 5
Global conversion for different bridge dimensions and Damkholer numbers.

Bridge-to-particle diameter ratio	Da: 0.005	Da: 1000
Benchmark bed	0.42%	92.71%
0.05	0.43%	92.64%
0.3	0.42%	92.65%

reported in Fig. 12, evaluated as

$$\omega_A = \frac{\int_S \rho \cdot \omega_A \cdot udS}{\int_S \rho \cdot udS} \tag{7}$$

Fig. 12 shows that also the axial profile is not affect by the local modification of the catalytic area. The reason of such low dependence of the system reactivity with respect to the local surface area modifications introduced by the bridges is in line with the fact that contact points are in quiescent regions of the bed and most of the fluid bypasses the bridge, as inferred from Fig. 13. This behavior is not affected by the presence of bridges, as it is clear by comparing Fig. 13a–c with b–d. As such, the exposed bridge area to the fluid is located in regions which are bypassed by most of the fluid, thus its contribution to the global conversion is negligible if

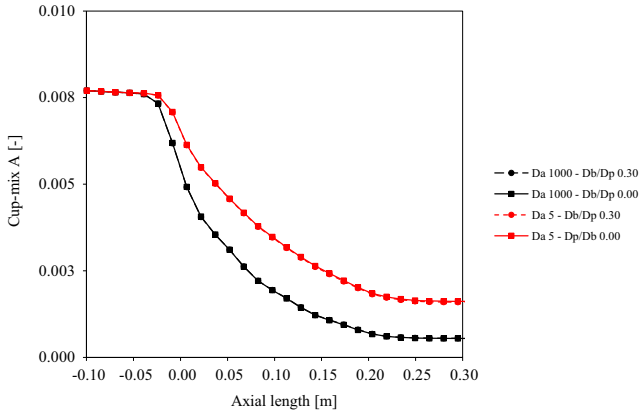

Fig. 12. Cup-mix axial profile for the reactant for different Damkholer numbers. Red lines correspond to Da=5. Black lines are Da=1000. Solid lines are the benchmark bed. Dashed lines are the bed with bridges. (For interpretation of the references to color in this figure legend, the reader is referred to the web version of this article.)

compared with the whole catalytic area of the spheres. To sum up, all the simulations demonstrate that, despite the relevant error on the catalytic area, the system reactivity is not strongly influenced by the bridges, as the result of the fact that the modifications of the geometry associated with the bridges are localized in stagnant regions. For this reason, the contribution of the bridges to reactivity is negligible.

3.2. *Random packed bed*

We extend now the analysis to a random packed bed, which is characterized by a much large number of contact points. To this aim, a random configuration of packed spheres is generated, as shown in Fig. 14. We perform the same analysis carried out for the regular packed bed, by investigating the effect of bridging on geometrical properties and conversion. On one side, the geometrical properties derived from the mesh at different bridge dimensions can be benchmarked with respect to the ones which can be calculated by the known number of spheres, as already done for the regular configuration. On the other side, the catalytic properties cannot be compared with the ideal situation of the exact description of contact points. Indeed, in this case, a packed bed without any bridges cannot be generated. The generation of a bed with an exact description of the contact points requires the spheres to be aligned along the pole-to-pole axis of the STL file, as described in Section 3.1. This situation cannot be exploited in a random packing due to: (i) the randomness and (ii) the high value of contact points per sphere. Therefore, on the basis of the previous analysis, we assess the effect of the bridge dimension by studying and checking the independence of the solution to the bridge-to-particle diameter ratio.

The mesh-independence study for the random packed bed reactor is carried out with the same operating conditions, reported in Tables 3 and 4, and the same criteria of the regular packed bed. The analysis is presented only for the bed with the smallest bridge-to-particle diameter ratio, but it has been carried out for all the beds. As shown in Fig. 15, the convergence is reached with a refinement level of 3 for TetGen (Si, 2007) (maximum cell volume of 10^{-5} m^3 and 6,857,769 cells). In Fig. 9b, the errors on the void fraction and the catalytic area as a function of the bridge-to-particle diameter ratio are reported. In agreement with what we found for the regular configuration, also in this case the void fraction turns out to be less affected by the presence of the bridges than the catalytic area. However, the errors are higher for the random configuration, because the local modifications of the

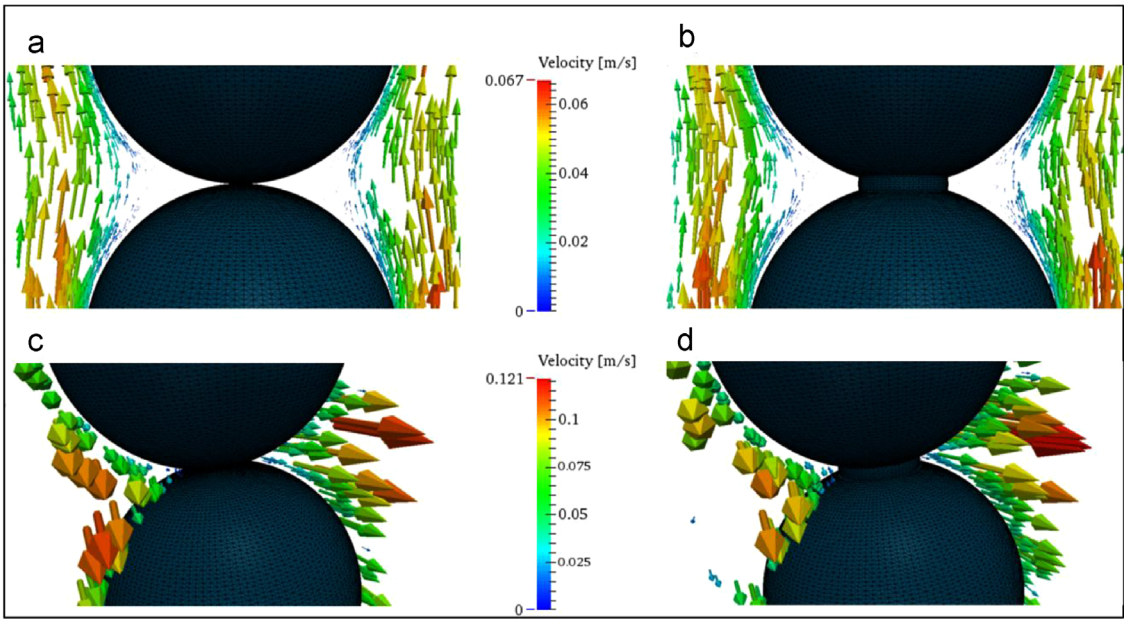

Fig. 13. Graphical visualization of the stagnant regions near the contact points: (a) beds without bridges configuration A. (b) Beds with bridges configuration A. (c) Beds without bridges configuration B. (d) Beds with bridges configuration B. Vectors represent the velocity in selected points of the domain and their dimension corresponds to the magnitude.

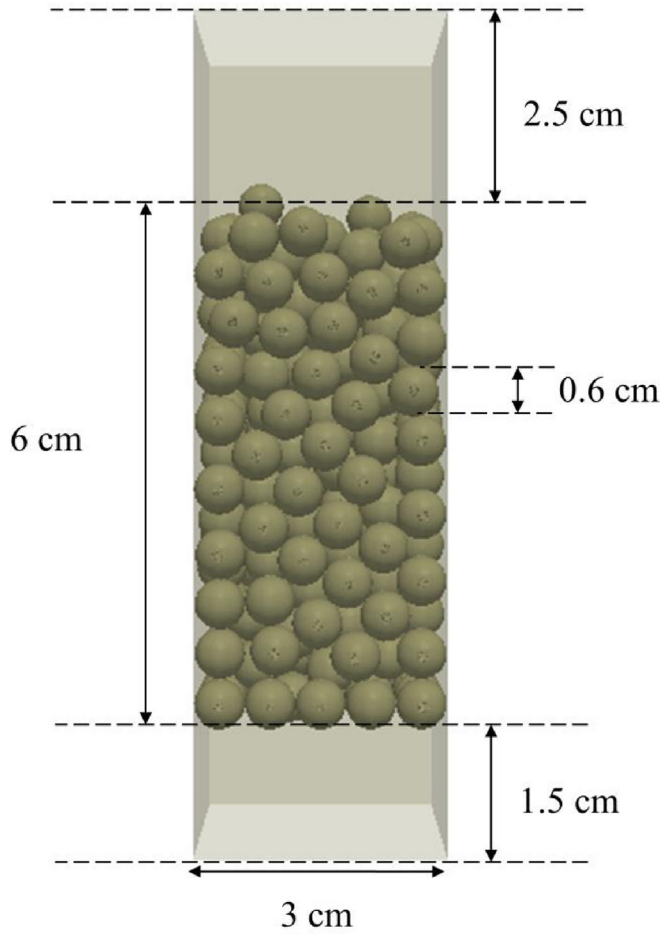

Fig. 14. Random packed bed dimensions.

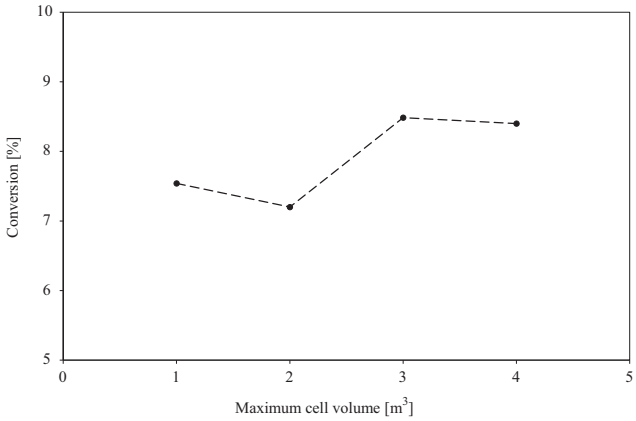

Fig. 15. Mesh independence analysis for random packed bed.

geometrical properties introduced by the bridges are related to the number of contact points per sphere. This value can be evaluated from the void fraction with the correlation proposed by Ridgway and Tarbuck (1967). For this random packed bed, the coordination number is ~7.5, instead of ~1 for the regular beds. For this reason, the catalytic area and the void fraction are more affected by the bridges in the random packed bed than in the regular packed beds.

Then, we investigated the effect of the bridge dimension on the conversion by performing reacting simulations using the same approach presented in Section 3.1. We selected a range of bridge-to-particle diameter ratio between 0.15 and 0.45. On one side, the lower bound is chosen on the basis of maximum acceptable skewness of the mesh compatible with numerical stability of the solution. On the other side, we used the limit found by Dixon et al. (2013) for describing the pressure drops as upper bound. Indeed, Dixon et al. (2013) clarified that using higher values of bridge-to-particle diameter ratio lead to errors in the description of the pressure drops and heat transfer. Moreover, they suggested that for error on the void fraction smaller than 1% the pressure drops and the flow field are not affected by the local modification. In Fig. 17 the dependence of the pressure drops on the bridge dimension is reported, showing that the pressure drops become bridge-independent for bridge-to-particle diameter ratio lower than 0.45. Thus, the error on the pressure drops can be considered

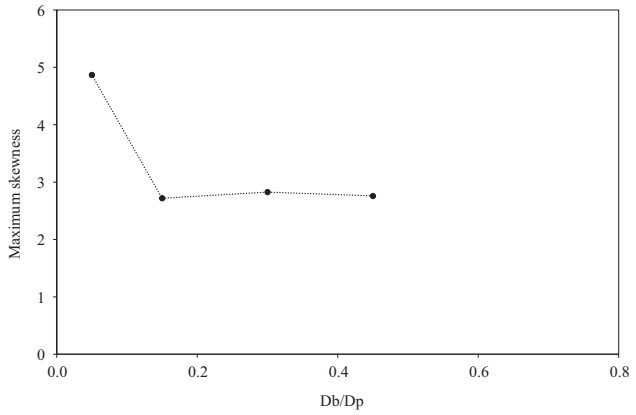

Fig. 16. Bridge dimensions effect on the max skewness for random bed.

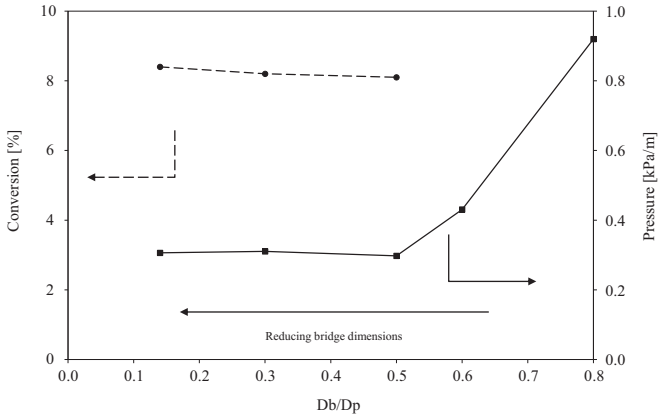

Fig. 17. Influence of bridge dimensions on pressure drops (solid line) and conversion (dashed line) for random packed bed.

acceptable until bridge-to-particle diameter ratio lower than 0.45, where the error on the void fraction is smaller than 1%.

The lower bound for the bridge-to-particle diameter ratio can be selected by analyzing the quality of the mesh. The skewness is the main issue related with the use of unstructured meshes and the description of the narrow area near the contact points because it leads to numerical problems during the calculation of the flow field. Indeed, all the methods described by Dixon et al. (2013), shown in Fig. 1, have been proposed to reduce these numerical problems. The effect of the bridge dimensions on the maximum skewness can be observed in Fig. 16. The maximum skewness is strongly related to the bridge dimensions and it sets a minimum value for the bridge-to-particle diameter ratio. As reported in Fig. 16, the maximum skewness reaches a constant value for a bridge-to-particle diameter ratio higher than 0.15. Thus the best approach to reduce the numerical issues related with the skewness is to create bridges with a bridge-to-particle diameter ratio higher than 0.15. Therefore, the conversion is analyzed for bridge-to-particle diameter ratio between 0.15 and 0.45.

Fig. 17 shows that the conversion is not affected by the presence of the bridges. This behavior of the random packed bed reactors was already observed for a regular packed bed. Also in this case the whole error on the catalytic area, associated to the bridge, is concentrated in stagnant regions of the reactors. For this reason, the conversion obtained for a bed with bridge-to-particle diameter ratio of 0.15 is the same of the reactor with a bridge-to-particle diameter ratio of 0.45.

This analysis leads to an interaction of the bridge dimensions, not only with the flow field, but also with the conversion. In fact, the correct description on the flow field corresponds to a correct description of the quiescent region near the contact points. Thus, the correct characterization of these regions allows reducing the effect of the error of catalytic area on the conversion.

In conclusion, this analysis leads to criteria for meshing packed bed reactors. The selection of the bridge dimensions becomes important for describing correctly all the phenomena occurring in these devices and for reducing the numerical problems. Therefore, we suggest that the minimum dimensions of the bridge can be selected by considering the maximum skewness of the mesh. On the contrary, the maximum dimensions can be chosen by analyzing the pressure drops. In fact, if the bridge dimension is small enough to not influence the flow fields, also the system reactivity can be correctly reproduced by this method of description of contact points.

4. Conclusions

This study has provided a systematic investigation of the treatment of the contact points for reactive CFD simulations of gas–solid packed of spheres. We identified a meshing protocol, which can be adopted to properly describe surface reactivity in packed bed reactors. In particular, we extended the bridge method to reacting simulations, which was previously selected as the most suitable one for correctly describing pressure drops and heat transfer in heterogeneous packed bed reactors. Our analysis of the quality of the mesh shows that lower values of bridge-to-particle diameter ratio result in an increased maximum skewness, which leads to important convergence problem for the numerical solution and thus a determines a minimum value for bridge-to-particle diameter required for the simulation. Moreover, the results demonstrate that the conversion is not remarkably influenced by the presence of the bridges for bridge-to-particle diameter ratio up to a limit that is the same reported in the literature for a correct description of the pressure drops. The reason of such an agreement is related to the flow field in proximity of the contact points, which turn out to be quiescent regions of the domain. As a result, the local modification of the surface area due to the introduction of the bridges does not substantially affect the overall reactivity.

Nomenclature

D_p: particle diameter [m]
D_b: bridge diameter [m]
a_v: specific area [m^{-1}]
A_C: catalytic area [m^2]
V_R: empty reactor volume [m^3]
N_s: number of spheres [dimensionless]
V_{mesh}: reactor volume estimated from the generated mesh [m^3]
A_{mesh}: catalytic area estimated from the generated mesh [m^2]
u: velocity [m/s]
k_C: kinetic constant [s^{-1}]
G: mass flux [kg/s m^2]

Greek letters

ε_V^{STL}: error on the volume of the STL file [%]
ε_A^{STL}: error on the surface area of the STL file [%]
ε_{void}: error on the void fraction [%]
ε_A: error on the catalytic area [%]
ω: mass fraction [dimensionless]
Γ_A: diffusivity of species A [m^2/s]
μ: mix viscosity [Pa s]

Dimensionless numbers

$\mathrm{Re} = \frac{GD_p}{\mu}$: particle Reynold number

$\mathrm{Da} = \frac{k_C D_p}{\Gamma_A}$:Damkholer number

Acknowledgments

Computational time at CINECA (Bologna, Italy) is gratefully acknowledged (Iscra C - HP10C1OBZB - MOTION).

Reference

Appel, C., Mantzaras, J., Schaeren, R., Bombach, R., Inauen, A., Tylli, N., Wolf, M., Griffin, T., Winkler, D., Carroni, R., 2005. Partial catalytic oxidation of methane to synthesis gas over rhodium: in situ Raman experiments and detailed simulations. P. Combust. Inst. 30, 2509–2517.

Augier, F., Idoux, F., Delenne, J.Y., 2010. Numerical simulations of transfer and transport properties inside packed beds of spherical particles. Chem. Eng. Sci. 65, 1055–1064.

Baker, M.J., Young, P.G., Tabor, G.R., 2011. Image based meshing of packed beds of cylinders at low aspect ratios using 3d MRI coupled with computational fluid dynamics. Comput. Chem. Eng. 35, 1969–1977.

Bu, S., Yang, J., Zhou, M., Li, S., Wang, Q., Guo, Z., 2014. On contact point modifications for forced convective heat transfer analysis in a structured packed bed of spheres. Nucl. Eng. Des. 270, 21–33.

Calis, H.P.A., Nijenhuis, J., Paikert, B.C., Dautzenberg, F.M., van den Bleek, C.M., 2001. CFD modelling and experimental validation of pressure drop and flow profile in a novel structured catalytic reactor packing. Chem. Eng. Sci. 56, 1713–1720.

Cundall, P.A., Strack, O.D.L., 1979. A discrete numerical model for granular assemblies. Géotechnique, 29.

Cuoci, A., Frassoldati, A., Faravelli, T., Ranzi, E., 2015. OpenSMOKE++: an object-oriented framework for the numerical modeling of reactive systems with detailed kinetic mechanisms. Comput. Phys. Commun. 192, 237–264.

Dixon, A.G., Nijemeisland, M., 2001. CFD as a design tool for fixed-bed reactors. Ind. Eng. Chem. Res. 40, 5246–5254.

Dixon, A.G., Nijemeisland, M., Stitt, E.H., 2013. Systematic mesh development for 3D CFD simulation of fixed beds: contact points study. Comput. Chem. Eng. 48, 135–153.

Dixon, A.G., Taskin, M.E., Nijemeisland, M., Stitt, E.H., 2010. CFD method to couple three-dimensional transport and reaction inside catalyst particles to the fixed bed flow field. Ind. Eng. Chem. Res. 49, 9012–9025.

Dudukovic, M.P., 2009. Frontiers in reactor engineering. Science 325, 698–701.

Eppinger, T., Seidler, K., Kraume, M., 2011. DEM–CFD simulations of fixed bed reactors with small tube to particle diameter ratios. Chem. Eng. J. 166, 324–331.

Freund, H., Bauer, J., Zeiser, T., Emig, G., 2005. Detailed simulation of transport processes in fixed-beds. Ind. Eng. Chem. Res. 44, 6423–6434.

Freund, H., Sundmacher, K., 2008. Towards a methodology for the systematic analysis and design of efficient chemical processes: Part 1. From unit operations to elementary process functions. Chem. Eng. Process.: Process. Intensif. 47, 2051–2060.

Freund, H., Zeiser, T., Huber, F., Klemm, E., Brenner, G., Durst, F., Emig, G., 2003. Numerical simulations of single phase reacting flows in randomly packed fixed-bed reactors and experimental validation. Chem. Eng. Sci. 58, 903–910.

Guardo, A., Coussirat, M., Recasens, F., Larrayoz, M.A., Escaler, X., 2006. CFD study on particle-to-fluid heat transfer in fixed bed reactors: convective heat transfer at low and high pressure. Chem. Eng. Sci. 61, 4341–4353.

Henderson, A., 2007. ParaView Guide, A Parallel Visualization Application. Kitware Inc..

Jasak, H., Jemcov, A., Tukovic, Z., 2007. OpenFOAM: a C++ library for complex physics simulations. Int. Workshop Coupled Methods Numer. Dyn., 1–20.

Jiang, P.-X., Xu, R.-N., Gong, W., 2006. Particle-to-fluid heat transfer coefficients in miniporous media. Chem. Eng. Sci. 61, 7213–7222.

Kee, R.J., Rupley, F.M., Miller, J.A., 1990. The Chemkin Thermodynamic Data Base. Sandia National Labs., Livermore, CA, USA.

Kloss, C., Goniva, C., Hager, A., Amberger, S., Pirker, S., 2012. Models, algorithms and validation for opensource DEM and CFD–DEM. Prog. Comput. Fluid Dyn., Int. J. 12, 140–152.

Lund, K.O., Nguyen, H., Lord, S.M., Thompson, C., 1999. Numerical correlation for thermal conduction in packed beds. Can. J. Chem. Eng. 77, 769–774.

Maestri, M., Cuoci, A., 2013. Coupling CFD with detailed microkinetic modeling in heterogeneous catalysis. Chem. Eng. Sci. 96, 106–117.

Magnico, P., 2003. Hydrodynamic and transport properties of packed beds in small tube-to-sphere diameter ratio: pore scale simulation using an Eulerian and a Lagrangian approach. Chem. Eng. Sci. 58, 5005–5024.

Ookawara, S., Kuroki, M., Street, D., Ogawa, K., 2007. High-fidelity DEM–CFD modeling of packed bed reactors for process intensification. In: Proceedings of European Congress of Chemical Engineering (ECCE-6), Copenhagen, pp. 16–20.

Raimondeau, S., Vlachos, D., 2002. Recent developments on multiscale, hierarchical modeling of chemical reactors. Chem. Eng. J. 90, 3–23.

Reid, R.C., Prausnitz, J.M., Poling, B.E., 1987. The Properties of Gases and Liquids.

Ridgway, K., Tarbuck, K., 1967. Random packing of spheres. Br. Chem. Eng. 12, 384.

Romkes, S.J.P., Dautzenberg, F.M., van den Bleek, C.M., Calis, H.P.A., 2003. CFD modelling and experimental validation of particle-to-fluid mass and heat transfer in a packed bed at very low channel to particle diameter ratio. Chem. Eng. J. 96, 3–13.

Schlereth, D., Hinrichsen, O., 2014. Comparison of a pseudocontinuous, heterogeneous 2D conductive monolith reactor model to a 3D computational fluid dynamics model. Ind. Eng. Chem. Res. 53, 11550–11556.

Si, H., 2007. TetGen. A Quality Tetrahedral Mesh Generator and Three-Dimensional Delaunay Triangulator. Version 1.

Soppe, W., 1990. Computer simulation of random packings of hard spheres. Powder Technol. 62, 189–197.

Touitou, J., Aiouache, F., Burch, R., Douglas, R., Hardacre, C., Morgan, K., Sá, J., Stewart, C., Stewart, J., Goguet, A., 2014. Evaluation of an in situ spatial resolution instrument for fixed beds through the assessment of the invasiveness of probes and a comparison with a micro-kinetic model. J. Catal. 319, 239–246.